Analysis of Sheet Metal Forming (Warm Stamping Process): A Study of the Variable Friction Coefficient on 6111 Aluminum Alloy

Shasha Dou [1,2,*]**, Xiaoping Wang** [1,*]**, Jason Xia** [2] **and Lisa Wilson** [3]

[1] College of Mechanical and Electrical Engineering, Nanjing University of Aeronautics and Astronautics, Nanjing 210016, China

[2] School of Mechanical Engineering, Yancheng Institute of Technology, Yancheng 224051, China; xiajs@ycit.edu.cn

[3] The Wolfson Centre, University of Greenwich, Gillingham ME4 4TB, UK; mengmin@ycit.cn

* Correspondence: lisadou@ycit.edu.cn (S.D.); levine@nuaa.edu.cn (X.W.); Tel.: +86-158-5107-9040 (S.D.)

Abstract: Aluminum alloy materials have been widely used in automobile, aerospace and other fields because of their low density, high specific strength and corrosion resistance. The process of the warm forming of aluminum alloy improves the formability of aluminum alloy sheets, reduces the deformation resistance and spring-back and improves the forming accuracy and quality of parts. For these reasons, it is frequently used. In this work, the effects of temperature, sliding speed and normal load on the friction coefficient of 6111 aluminum alloy were studied by using a CFT-I (Equipment Type) friction tester under boundary lubrication conditions. The surface morphology of the sample after the friction test was observed by optical microscopy. The results show that the surface quality of aluminum alloy is better at 200 °C, which was used as the temperature in the experiments. According to the test measurement results, the friction coefficient increases with the increase in temperature and decreases with the increase in sliding speed and normal load. Variable friction coefficient models of sliding speed and normal load were established. Using the optimal parameter combination as the simulation parameter, the established variable friction coefficient models were input into numerical simulation software, and two sets of comparative simulations were established. The thickness distribution of the sheet material obtained through the simulation was compared with the actual test measurement. Further verification was carried out through the amount of spring-back. The results show that the thickness distribution and spring-back of the sheet obtained by the variable friction coefficient model are closer to the actual measurements (the error of the spring-back angle decreased from more than 20% to less than 10%), which verifies the reliability and accuracy of the variable friction coefficient model.

Keywords: aluminum alloy; warm forming; friction coefficient; process parameters; numerical simulation

1. Introduction

With the continuous development of lightweight technology, aluminum alloy materials are being more widely used in automotive, aerospace and other fields than ever before. This is because of the low density, high specific strength and corrosion resistance of aluminum alloy materials. However, when compared with steel materials, aluminum alloy demonstrates poor plasticity at room temperature, as well as difficulties for pressing a body panel with a complex shape. In addition, defects such as spring-back and fracture are prone to occur after the sheet metal stamping process. In many cases, it is difficult to guarantee the dimensional accuracy of parts, and the qualification rate of parts processed is comparatively low, which production costs [1].

Warm metal forming generally refers to the forming process in which the material is heated to a temperature below the dynamic recovery or recrystallization temperature through the heat transfer of the furnace or die. Under the warm forming condition, the elongation of the aluminum alloy sheet can reach levels between 20% and 25%, the strength of stamping parts increases, the spring-back decreases and the forming accuracy improves [2]. According to the temperature between the sheet metal and the die, warm forming can be divided into isothermal forming and non-isothermal forming. In the process of isothermal forming, the temperatures of the sheet metal and the die remain basically the same, which can improve the plasticity of the sheet metal and the uniform distribution of the wall thickness of parts. However, the warm forming process imposes higher demands on equipment, resulting in increased production cost and difficulty, and the anti-concave performance of parts can be poor. In the non-isothermal forming process, there is a specific temperature difference between the sheet metal and the die. During the stamping process, heat is transferred between the sheet metal and the die. The temperature of the sheet metal changes in real time, so it is widely used in the actual production process [3]. El Fakir et al. [4] put forward a new integrated processing technology that combines warm forming and heat treatment, called solution heat treatment forming cold die quenching, which can realize synchronous forming and quenching. This effectively solves the difficult problem of complex part processing while ensuring the plasticity of aluminum alloy.

Finch and Wilson et al. [5,6] carried out experimental research on aluminum alloy after annealing and tempering in a cylinder and square box. The results showed that the drawing properties of the aluminum alloy sheet were improved at 200 °C, and the shape of the formed parts had no effect on the sheet properties. Ayres and Wenner [7] studied the influence of forming temperature and punch speed on the forming limit of 5182 aluminum alloy through a punch bulging experiment. It was found that the forming limit of the sheet metal increased significantly with the increase in temperature and decrease in punch speed, and the results showed the strain distribution of the material tended to be within a reasonable range. D. Li et al. [8] studied the mechanical properties of 5182, 5754 and 6111 aluminum alloys at different temperatures and strain rates through a uniaxial tensile test. The results showed that the elongation of the sheet metal increased, corresponding to the increase in temperature and the decrease in strain rate, and the effect of temperature on the strain rate sensitivity coefficient was more pronounced. V.M. Simões [9] reported that the punch speed had a significant influence on the success of the sheet metal warm forming of aluminum alloys, and formability and spring-back remained stable or improved with the increase in punch speed.

Lee et al. [10] also studied the influence of lubricant viscosity and surface roughness on the friction coefficient, established a friction model and calculated the relationship between the friction coefficient, lubricant viscosity and surface roughness by the least squares method. The Equation is as follows:

$$\mu = \frac{23.2}{104.5 + \nu^{0.98}} - 5.3 \times 10^{-6}(\nu - 56.6)^2 + 0.24(\lambda - 0.76)^2 - 0.112 \tag{1}$$

where ν is the lubricant viscosity and λ is the surface roughness.

IM.Y.T. et al. [11] modified the classical Coulomb friction model by using the finite element method and an arctangent function and introduced the relative slip velocity. The modified model can maintain continuous friction stress on the boundary, and its shear friction model is as follows.

$$\tau = mk\left\{\frac{2}{\pi}\arctan\left(\frac{|u_r|}{u_0}\right)\right\}\frac{u_r}{|u_r|} \tag{2}$$

Y.Z. Zhao et al. [12] studied the relationship between load and the friction coefficient under boundary lubrication conditions and established a variable friction coefficient model based on different interface loads.

$$\mu = 0.133(p/1.03)^{-0.177} \tag{3}$$

S.S. Dou [13] studied the influence of sliding speed and interface load on the friction coefficient under the boundary lubrication condition and established a comprehensive variable friction coefficient model with variable speed and variable load:

$$\mu = \frac{1.849P + 13.3}{(P + 2.446)(0.9193P + 1.467 + v)} \tag{4}$$

where P is the interface load and v is the sliding speed.

Currently, there is no singular conclusion about the friction problem in the warm forming of aluminum alloy, as the stamping process for an aluminum alloy sheet is a highly nonlinear changing process, and the friction behavior between aluminum alloy and the die is exceedingly complex. It is important to study the friction characteristics of aluminum alloy warm forming to improve the accuracy of CAE (Computer Aided Engineering) simulation. The influence of the initial forming temperature, positive pressure (normal load) and sliding speed on the friction coefficient between 6111 aluminum alloy and an H13 die steel surface was investigated by using a CFT-I multifunctional material surface comprehensive performance tester (Zhongke Kaihua Technology Development Co., Ltd., Lanzhou, China) under boundary lubrication conditions. The surface morphology of 6111 aluminum alloy after a friction experiment with H13 die steel was observed and analyzed using a microscope. The influence law of multiple factors on the friction coefficient under different conditions was analyzed, leading to a friction model being established. In addition, the model of the variable friction coefficient was also established through experimentation, which is proved to improve simulation accuracy.

2. Materials and Methods

2.1. Materials

In this test, 6111-T4 aluminum alloy with a thickness of 1 mm was used. Among the 6000-series alloys, 6111 aluminum alloy has the highest strength and has wide application prospects across the automotive industry [14]. Its chemical composition is shown in Table 1.

Table 1. Chemical composition of 6111 aluminum alloys (wt.%), data from [14].

Components	Si	Fe	Cu	Mg	Zn	Ti	Cr	Mn	Al
Mass fraction	0.75	0.40	0.50–0.90	0.70	0.10	0.10	0.10	0.15–0.45	96.5–97.2

H13 hot working die steel was used as the friction pair in the friction test, and its hardness was 55 HRC (Rockwell Hardness) after quenching and tempering. The test sample and fixture are shown in Figure 1a, and the aluminum alloy sample after the friction test is shown in Figure 1b. Abrasive paper was used to grind and polish the working surface of the die block, and the contact surface state of the actual stamping process was simulated. The contact surface of the aluminum alloy and the die was measured and observed through the use of an optical microscope, and its surface roughness Ra was recorded as 0.2–0.6 μm and 0.8–1.3 μm.

2.2. Lubrication

Firstly, the contact surfaces between the H13 die steel and aluminum alloy were polished and then put into the beaker containing acetone and anhydrous ethanol for ultrasonic cleaning and dried with a blower. Through calculation, a certain amount of molybdenum-disulfide lubricant and boron-nitride (BN) high-temperature anti-oxidation agent were sprayed evenly on the surface of the sheet to form a certain thickness of oil film. The usage calculation is based on the ratio of the minimum oil film thickness to friction surface roughness λ—λ > 2 for fluid lubrication, λ < 1 for boundary lubrication and 1 < λ < 2 for mixed lubrication.
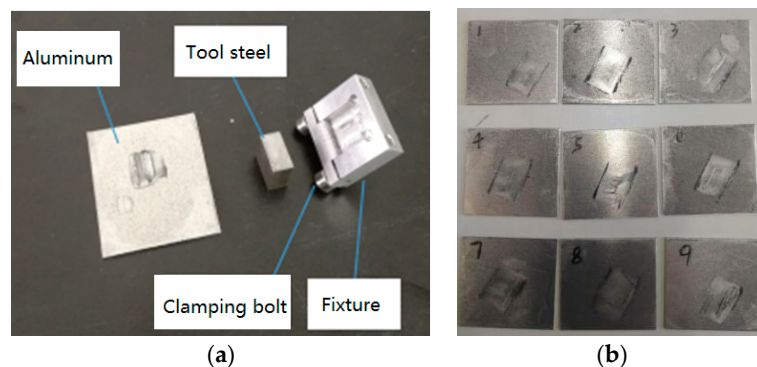
Figure 1. Diagram of the friction test sample. (**a**) Friction objects; (**b**) Aluminum plate samples.

2.3. Test Equipment

The experiment was carried out on a CFT-I multifunctional material surface comprehensive performance tester (shown in Figure 2). In this device, the heating furnace is fixed on the reciprocating motion test platform, which is heated by a resistance wire and controlled by a temperature controller, and the required temperature is output to the workbench. The sheet is fixed in the heating furnace (Zhongke Kaihua Technology Development Co., Ltd., Lanzhou, China) through the fixture for heating, and the test is carried out after the sheet reaches the set temperature for 5 min. The reciprocating platform with the heating furnace and sheet sample moves along the x-axis direction, driven by an AC servo motor (Zhongke Kaihua Technology Development Co., Ltd., Lanzhou, China). The loading structure of the H13 block is in the upper part and in a relatively static state. When loading the sample or applying a load, the H13 block can move up and down along the Z-axis with the lifting platform. After reaching the set temperature, the plate–plate friction and wear test is conducted after holding for 5 min. To ensure that the temperature of the sample corresponds to the real environment, the temperature controller is divided into two stages: the heating stage, when the heating furnace temperature rises rapidly to the system temperature, and the insulation stage, when the plate is insulated, the z-axis lifts and the translation table loading the mold sample drops in the vertical direction. After the die comes into contact with the sheet metal, the normal load is continuously applied to the setting value. In the process of measurement, the loading structure of H13 steel remains relatively static. The reciprocating platform with the heating furnace and aluminum alloy disk sample moves reciprocally along the x-axis direction, driven by the AC servo motor.
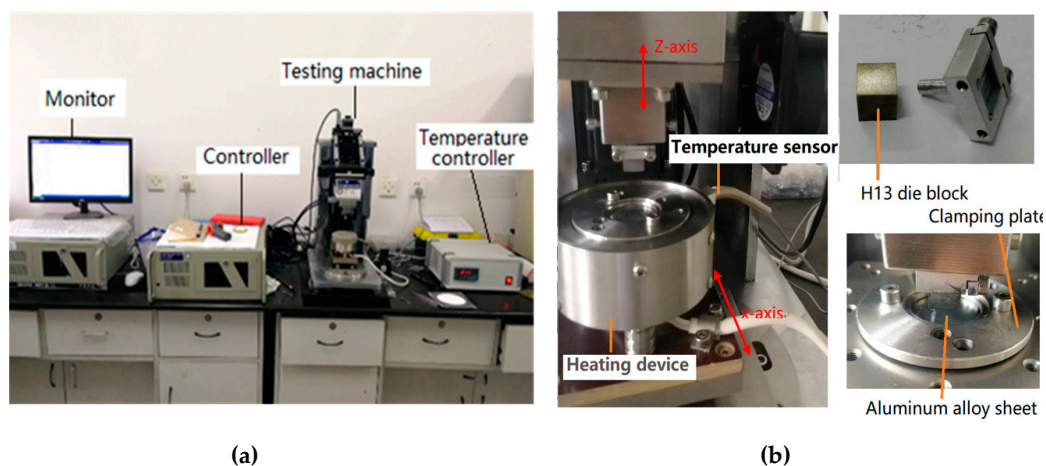
Figure 2. CFT-I multifunctional material surface comprehensive performance tester. (**a**) Disk–pin friction test principle; (**b**) Temperature control table.

During the friction process, the force sensor records the normal load and tangential friction force in real time, transmitting measured data to the computer. The real-time friction coefficient μ is calculated by Coulomb's law Equation (5):

$$\mu = \frac{F_x}{F_z} \tag{5}$$

where F_x is the tangential friction force with the unit N, and F_z is the normal friction force with the unit N.

2.4. Experimental Arrangement

The purpose of this friction experiment was to study the friction characteristics between H13 tool steel and 6111 aluminum alloy under different process parameters. The friction problem in the warm forming process for aluminum alloy, as referenced earlier, is very complex. The influence of the initial temperature, normal load and sliding speed on the friction characteristics of aluminum alloy are the main points of focus. The experimental parameters are shown in Table 2.

Table 2. Parameter settings of 6111 aluminum alloy for the friction test.

Sheet Temperature (°C)	Load Fz (N)	Sliding Speed Vx (mm/s)	Running Stroke L (mm)	Contact Conditions
25	10	20	5	
100	20	30	5	
150	30	40	5	Boundary lubrication
200	40	50	5	
250	50	60	5	

3. Results

*3.1. Effect of Sheet Temperature on Friction and Wear Behavior of Materials*

The friction coefficient can be used to measure the friction performance of materials during the forming process. The friction coefficient can reflect the friction force needed to overcome friction and slide up the deforming material. The larger the friction coefficient, the worse the friction performance of the material [15]. The sensor system monitors and records the positive pressure and horizontal friction in real time. The measured data are transmitted to the computer software synchronously, and the friction coefficient is calculated by Equation (5). Under the boundary lubrication condition and for a sliding speed of 30 mm/s and a normal load of 20 N, the variation curve of the interfacial friction coefficient over time for the 6111 aluminum alloy at different temperatures is shown in Figure 3a.

As seen in Figure 3a, the friction coefficient increases rapidly within the first few seconds and then decreases and finally slowly rises to a relatively stable fluctuation state. This is because more tangential force is needed to overcome the static friction force between the die block and the sheet metal at the beginning of the process, and the sliding friction force is smaller than the maximum static friction force. At the peak value of the friction coefficient, the maximum static friction occurs. After that, relative sliding occurs between the tool and the sheet metal, resulting in a slight decrease in the friction coefficient. It can be seen from the peak value of the curve that the maximum static friction needed to overcome increases with the increase in the temperature, and this is because the material softens with the increase in temperature, leading to decreases in the strength and hardness of the plate [16]. Under the conditions of the same sliding speed and loading load, the micro-convex bodies on the surface of the material are embedded in each other, which increases the contact area and makes the tangential friction force increase significantly. At the same time, given the increase in temperature, the viscosity of the lubricant on the surface of aluminum alloy decreases, and the ability of the lubricating oil film to resist load decreases. However, the oxide film on the surface of aluminum alloy remains relatively brittle and hard. After the oxide film is broken, the friction between friction

pairs is increased, and the friction coefficient increases, which is consistent with actual experience [17]. The friction coefficient curve can be divided into two stages: the rapid rise in the friction coefficient and the stable fluctuation stage.

The actual production cycle of sheet metal stamping is fast. In order to make the test results better reflect the actual stamping process, the friction coefficient changes in the running-in stage are consistent with those of the actual situation. As seen in Figure 3a, at the beginning, the curve is fluctuating. After 5 s, the friction coefficient tends to be stable, not oscillating violently. Therefore, the average value of the friction test results from 5 to 15 s was taken as the effective friction coefficient, and each group of experiments was repeated three times. The effective friction coefficient at different temperatures is shown in Figure 3b.

(a)   **(b)**
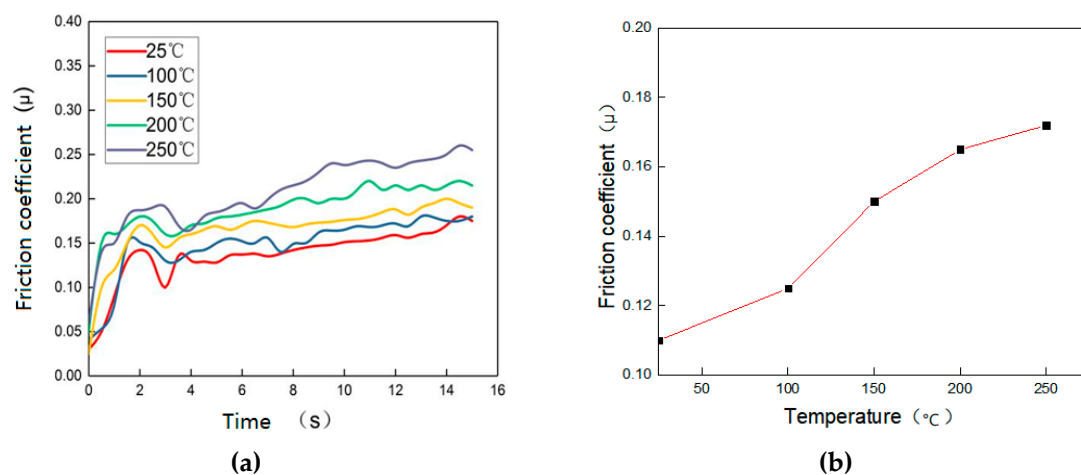
Figure 3. The fluctuation curve of the friction coefficient with sliding stroke in boundary lubrication: (**a**) Variation curves of the friction coefficient with time under different temperatures; (**b**) Experimental friction coefficients at different temperatures.

It can be seen from the figure that the effective friction coefficient will increase gradually in line with the increase in temperature. When the temperature increases from room temperature to 200 °C, the friction coefficient increases rapidly with the increase in temperature. At 200 °C, the friction coefficient is about 0.155. Above 200 °C, the friction coefficient increases slowly, corresponding to the increase in temperature.

For a stamping speed of 30 mm/s and a normal load of 20 N, the surface morphologies of the aluminum alloy at different temperatures were observed with a laser scanning microscope vk-x100 (KEYENCE, Osaka, Japan), as shown in Figure 4.

As shown in Figure 4a, the surface is relatively stable with a small number of scratches and many fine abrasive particles, so abrasive wear and furrow wear occurred. As seen in Figure 4b,c, the scratches on the surface became increasingly significant with the increase in test temperature, with scratch depth also increasing. The number of fine particles on the surface is seen to have decreased, indicating that the friction mechanism was mainly plow wear.

As seen in Figure 4e, there were many adhesion pits on the surface of the aluminum alloy, and the surface metal was peeled off and torn, resulting in serious adhesive wear. The original sheet, as shown in Figure 4f, had fewer surface scratches on it.

By analyzing the surface morphology of the 6111 aluminum alloy at different temperatures and considering the production cost and heating conditions in actual production, the warm forming temperature was determined to be 200 °C.
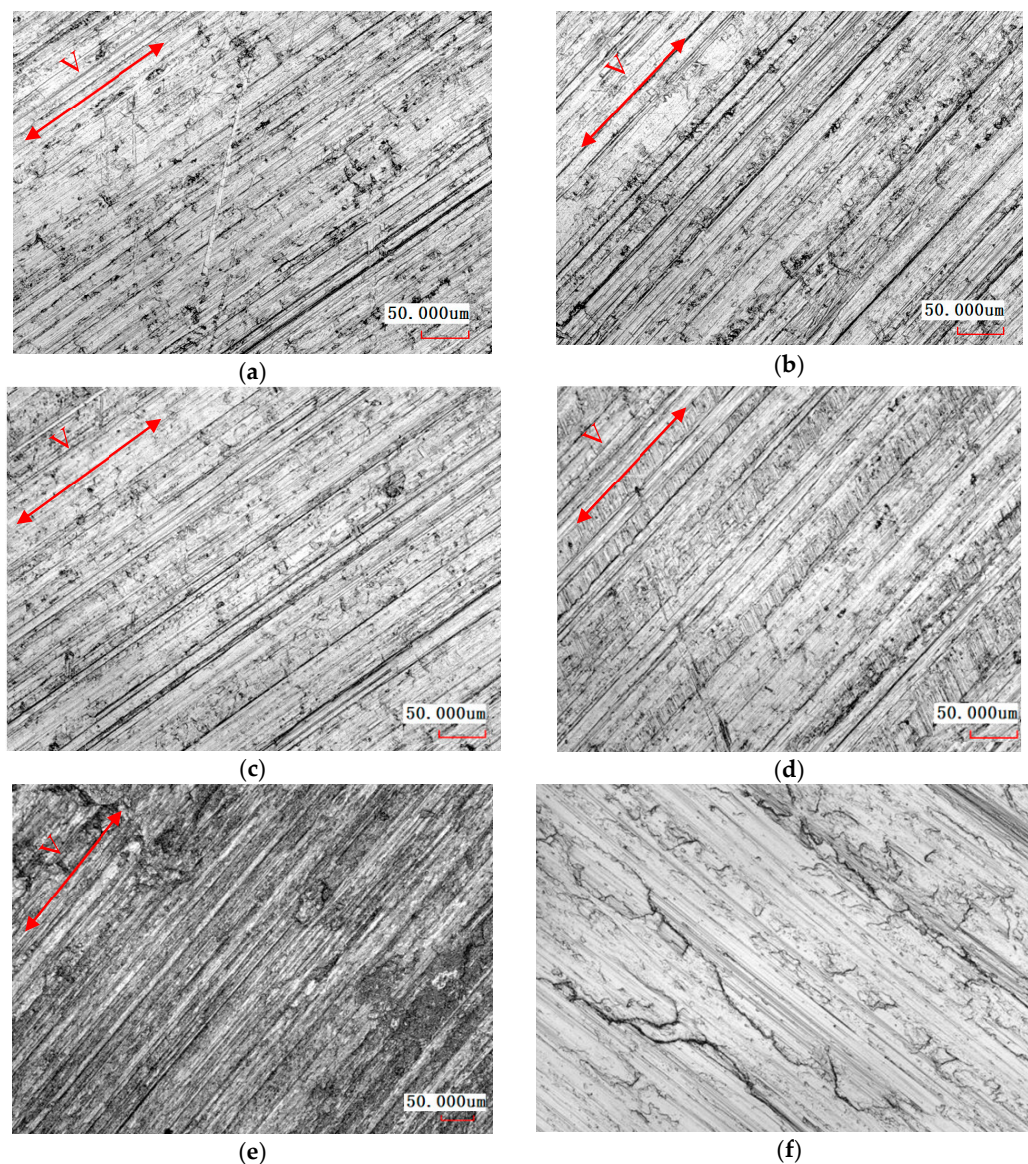
Figure 4. Surface morphology at different temperatures. (**a**) T = 25 °C; (**b**) T = 100 °C; (**c**) T = 150 °C; (**d**) T = 200 °C; (**e**) T = 250 °C; (**f**) Original sheet.

3.2. Effect of Sliding Speed on Friction and Wear Behavior of Materials

Under boundary lubrication conditions and for a temperature set at 200 °C and a load of 20 N, the change trend curve over time of the interface friction coefficient between the 6111 aluminum alloy and H13 tool steel at different sliding speeds is shown in Figure 5. It can be seen from Figure 5a that the friction coefficient curves under different sliding speeds have a common feature: during the first few seconds, the friction coefficient increases rapidly to a larger value and then decreases slightly, and it then enters a relatively stable fluctuation stage. This is because, with the increase in the sliding speed, the micro-convex bodies on the contact surface of the aluminum alloy sheet and the tool cannot be embedded in the pits in time, which reduces the actual contact area, reducing the friction coefficient of the sheet metal. On the other hand, the increase in the sliding speed causes the shear speed of the bonding points on the contact surface to decrease, and the number of shear bond points per unit time increases. Therefore, the friction coefficient between the 6111 aluminum alloy and the H13 steel surface decreases with an increase in sliding speed.
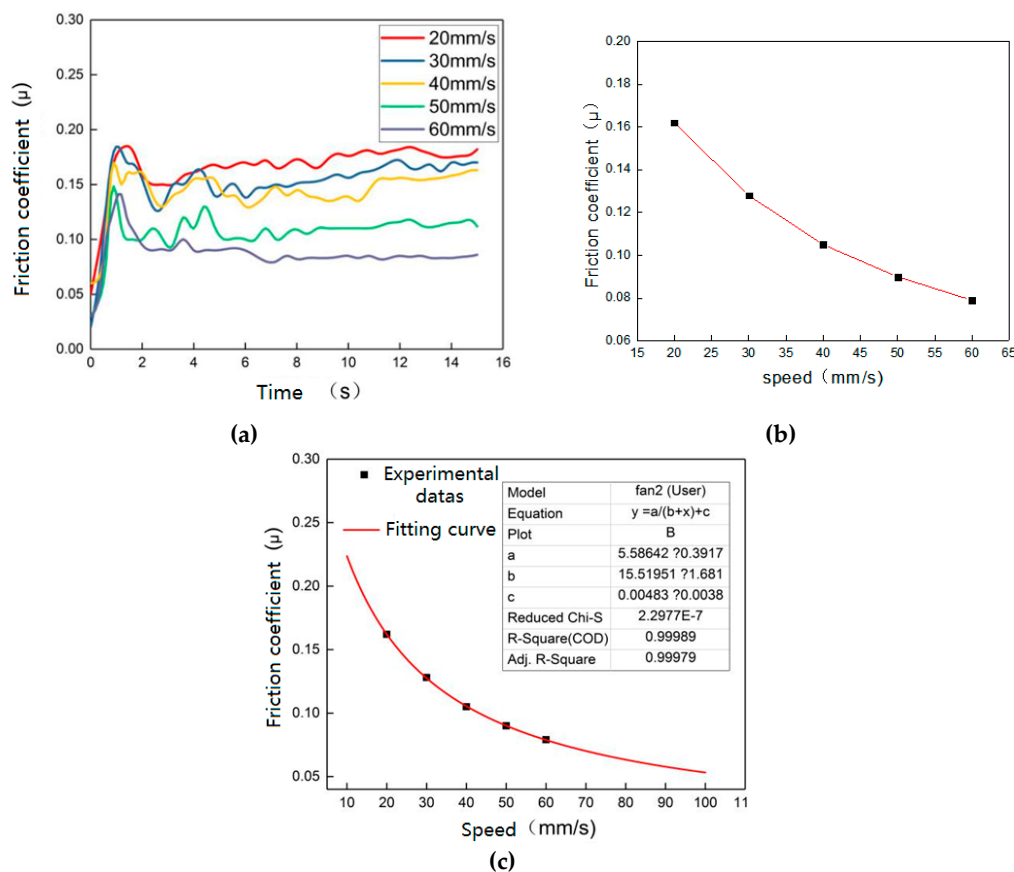
Figure 5. The fluctuation curve of the friction coefficient according to sliding speed: (**a**) Variation curves of the friction coefficient over time under different speeds; (**b**) Experimental friction coefficients under different speeds; (**c**) Inverse function fitting curve.

The experimental results indicate that the effective friction coefficients of the material contact interface are 0.162, 0.128, 0.105, 0.09 and 0.079 when the sliding speeds are 20, 30, 40, 50 and 60 mm/s, respectively. The curve of the friction coefficient change with velocity is shown in Figure 5b. It can be seen from Figure 5b that when the speed is less than 40 mm/s, the friction coefficient decreases rapidly with the increase in sliding speed; when the speed is greater than 40 mm/s, the rate of decrease of the friction coefficient with the increase in sliding speed gradually slows down. The change trend of the curve conforms to the characteristics of the inverse function, and the expression is shown in Equation (6):

$$\mu = \frac{a}{v+b} + c \tag{6}$$

where μ is the friction coefficient; v is the sliding speed; and a, b and c are constants.

The inverse function curve of the friction coefficient under different sliding speeds was fitted with the Origin software. As seen in Figure 5c, the values of the function constants of a, b and c are 5.586, 15.52 and 0.005, respectively. The fitting degree of the function curve is 0.9998, so the curve can better reflect the variable relationship between the sliding speed and friction coefficient. The fitting function model was built and is shown in Equation (7).

$$\mu = \frac{5.586}{v+15.52} + 0.005 \tag{7}$$

In order to verify the effectiveness of the friction coefficient model, five groups of sliding speeds, with speeds of 15, 25, 35, 55 and 70 mm/s, were selected for test measurements. The five groups of sliding speed values were correspondingly substituted into Equation (7). The actual measurement

and function prediction calculation results are shown in Table 3. By contrast, the error between the experimental value of the friction coefficient μ_1 and the prediction result of the function model μ_2 was less than 5%. The model can effectively describe the relationship between the friction coefficient and the sliding speed in the actual stamping process, which verifies the effectiveness of the friction model.

Table 3. Friction coefficient measurement and function model prediction.

| Speed (mm/s)	15	25	35	55	70
μ_1 (measured value)	0.194	0.145	0.112	0.082	0.073
μ_2 (calculated value)	0.188	0.143	0.116	0.084	0.07
Error rate (%)	3.09	1.38	3.57	2.44	4.11

Under the conditions of a temperature of 200 °C and a load of 20 N, the microstructures of the aluminum alloy surface with different sliding speeds of 20, 30, 50 and 60 mm/s were observed, as shown in Figure 6. It can be seen in Figure 6a that there was a small number of fine abrasive particles on the surface, and there was a large number of deep scratches, as well as obvious spalling marks, mainly furrow wear and adhesive wear. Figure 6b shows that the adhesion pits and scratches on the surface of the 6111 aluminum alloy became shallower, and the number of scratches was reduced. Figure 6c reveals that the scratches on the surface were increased in number, and a few scratches appear to have been deepened, with a few adhesion pits on the surface. As seen in Figure 6d, when the speed increased to 60 mm/s, the surface was relatively stable, the scratches were reduced and not as deep, and the adhesion pits were flattened. In conclusion, with an increase in sliding speed, the actual contact area between 6111 and H13 decreases, thus reducing the friction coefficient.

(a)

(b)

(c)

(d)
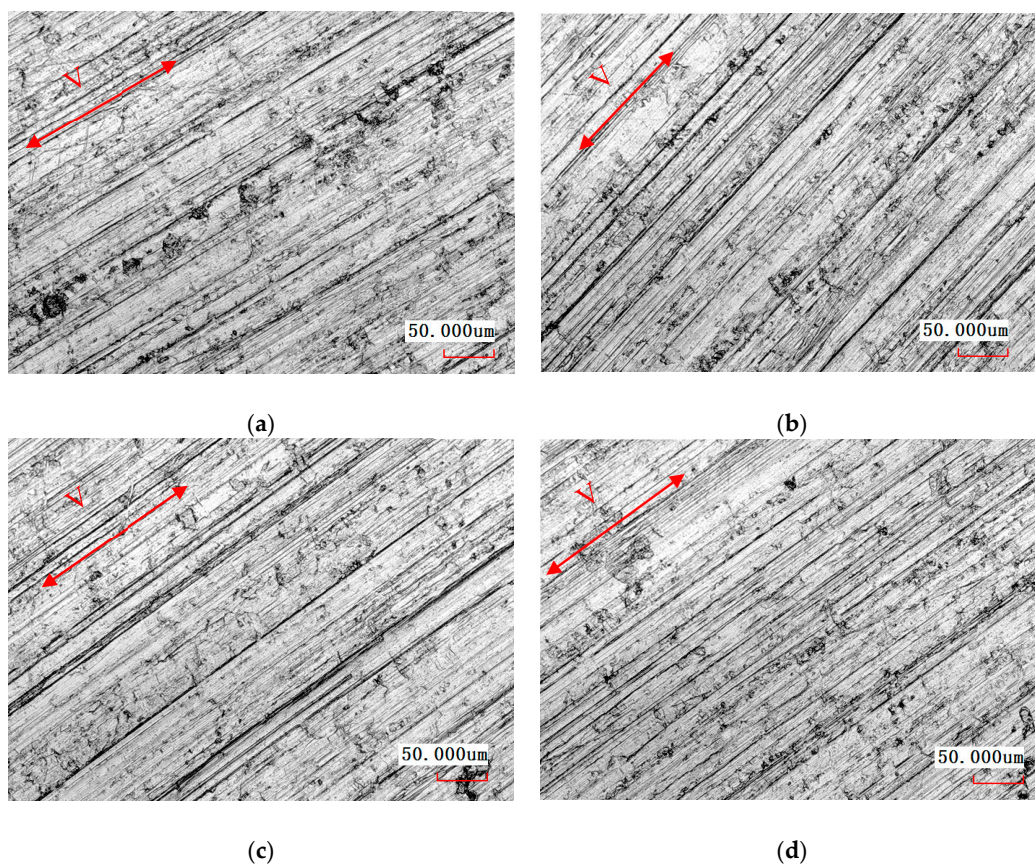
Figure 6. Surface morphology under different sliding speeds. (**a**) 20 mm/s; (**b**) 30 mm/s; (**c**) 50 mm/s; (**d**) 60 mm/s.

3.3. Effect of Normal Load on the Friction Behavior of Materials

During the actual stamping process, normal loading refers to normal pressure on the pressing plate, which affects friction and wear by changing the contact area and deformation state [18]. Under the boundary lubrication condition and for an initial temperature of 200 °C and a sliding speed of 30 mm/s, the curve of the friction coefficient varying with time under different normal loads is shown in Figure 7. As shown in Figure 7a, the friction coefficient first rises sharply and fluctuates greatly, and then, it decreases gradually. As time goes on, the curve fluctuates gently and reaches a relatively stable fluctuation state, which is the friction coefficient decreasing with the increase in load.
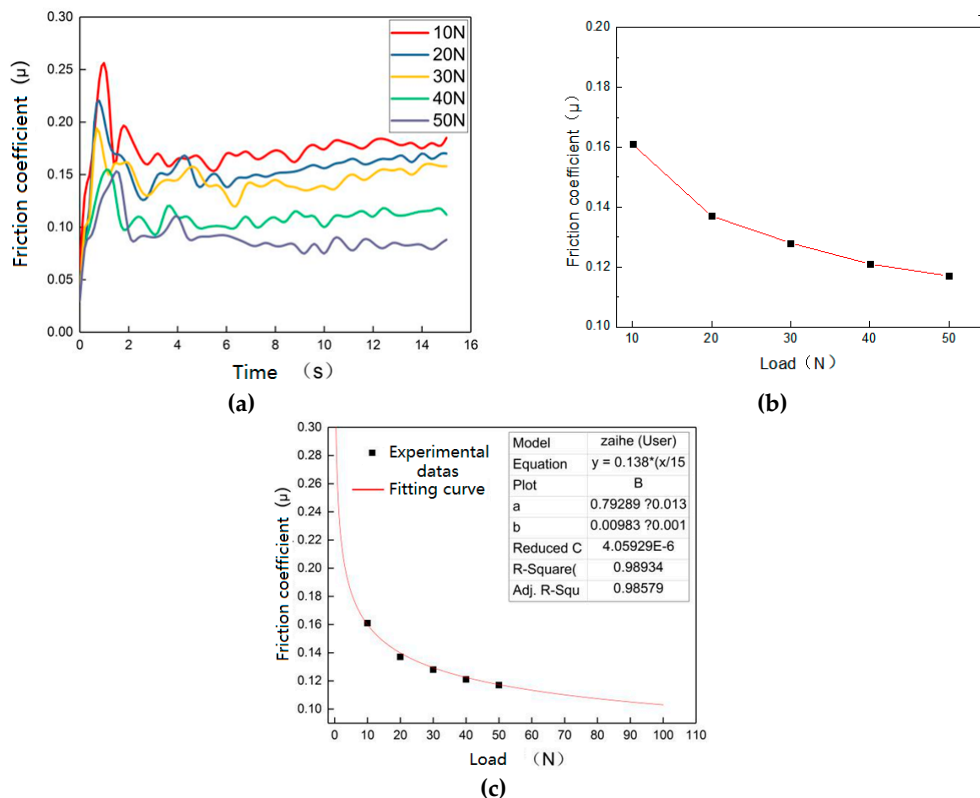
Figure 7. Friction coefficient curve under different loads: (**a**) Variation curves of the friction coefficient over time under different loads; (**b**) Experimental friction coefficients at different loads; (**c**) Fitting curve of the friction coefficient with load.

The fitting curve of the friction coefficient with load is shown in Figure 7c. It can be seen from the figure that the friction coefficient decreases with the increase in load, and the change trend of the curve is consistent with the tribological principle [19].

According to Y.Z. Zhao et al. [12], the new variable friction coefficient model was established, as shown in Equation (8):

$$\mu = \mu_0 \left(\frac{F}{F_o}\right)^{a-1} + b \tag{8}$$

where F is the normal load, F_0 is the reference load, μ_0 is the measured friction coefficient and α is the model index ($F_0 > 0$, $0.5 \le \alpha \le 1$).

Under the boundary lubrication condition, the load corresponding to a friction coefficient close to 0.15 was selected as the reference load, that is, $F_0 = 15$, $\mu_0 = 0.138$. The test results were fitted with the Origin software, and the fitting curve is shown in Figure 7c.

From the fitting, the values of a and b are 0.793 and 0.01, respectively, and the fitting degree is 0.9858, which shows that the model can better reflect the variable relationship between the load and

friction coefficient. The functional relationship between the friction coefficient and interface load is as follows.

$$\mu = 0.138(F/15)^{-0.207} + 0.01 \tag{9}$$

Five groups of normal loads of 15, 25, 45, 55 and 65 N were selected in order to verify the validity of the model. The values of the five groups of normal loads were substituted into Equation (9). The actual measurement and function prediction calculation results are shown in Table 4.

Table 4. Friction coefficient measurement and function model prediction.

Load (N)	15	25	45	55	65
μ_1 (Measured value)	0.138	0.125	0.115	0.108	0.104
μ_2 (Calculated value)	0.148	0.134	0.120	0.115	0.112
Error rate (%)	7.25	8.57	4.26	6.90	7.50

As seen from the data in Table 4, the error rates between the measured value and the predicted result are less than 9%. Thus, the friction coefficient model is verified for the effectiveness in the stamping process.

For a temperature of 200 °C and a sliding speed of 30 mm/s, the surface micro-morphology of the 6111 aluminum alloy under different normal loads is shown in Figure 8.
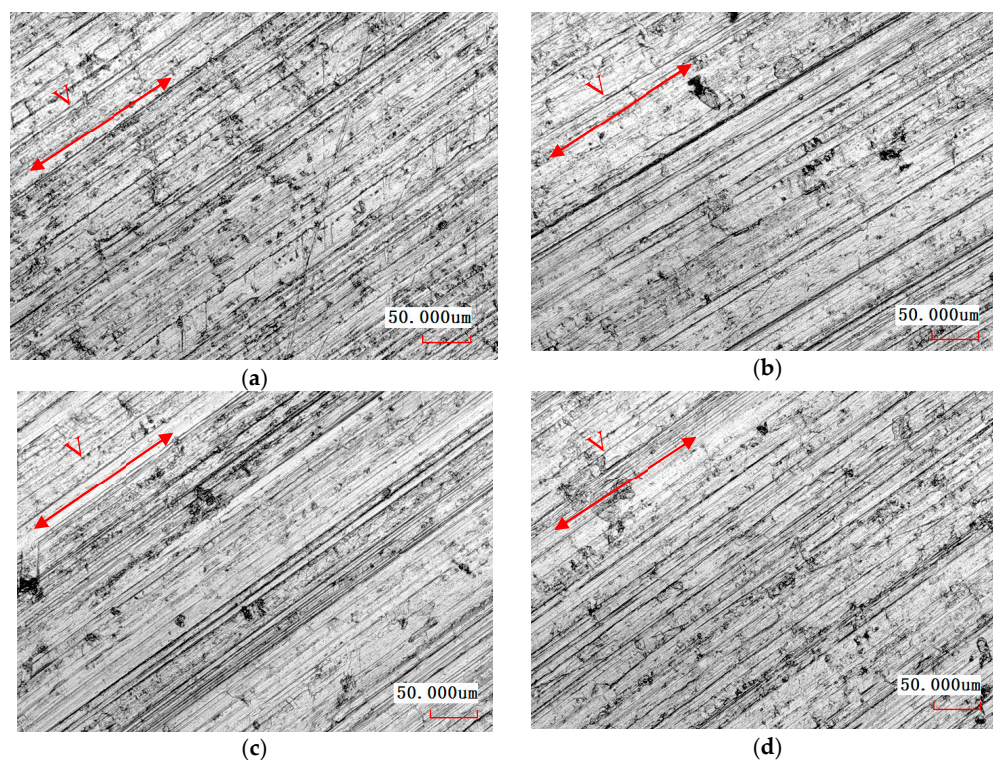
Figure 8. Surface morphology under different normal loads: (**a**) 10 N; (**b**) 20 N; (**c**) 40 N; (**d**) 50 N.

As seen in Figure 8a, there were slight scratches on the surface, which were caused by relative sliding between the convex peak on the H13 steel surface and the concave valley on the 6111 aluminum alloy surface, resulting in furrow wear. From Figure 8b, it can be seen that the scratches on the surface decreased slightly, and there were some small adhesion pits; that is, the friction mechanism was mainly abrasive wear and adhesive wear. It can be seen in Figure 8c that the small adhesion pits became shallow, and local furrows were deepened. Figure 8d shows that when the normal load was increased to 60 N, the scratch on the surface increased and deepened, and slight peeling marks can be observed.

4. Discussion

In order to test the effectiveness of the variable friction model in predicting the numerical simulation of sheet metal stamping, the friction model was inputted into the DYNAFORM 5.9 software (ETA CO, US) to simulate the thickness distribution within the U-bending part. For the spring-back analysis of hot stamping, "6*MAT_THERMAL_ISOTROPIC_TD_LC" was selected as the material models of the sheet and tooling, which are non-isothermal analysis models.

Under the warm forming condition, the stamping speed is 2000 mm/s, the blank holder force is 30 KN and the friction coefficient is 0.12. The friction coefficient is set as the variable friction coefficient model and input with the table. The friction of the blank holder is controlled by the variable friction coefficient model for the load, and the friction between the sheet metal and the punch and die is controlled by a variable friction coefficient model for the speed. The simulation process parameters are shown in Table 5.

Table 5. The simulation process parameters.

Sheet Temperature (°C)	Holding Time (min)	Tooling Temperature (°C)	Transfer Time (s)	Blank Holder Force (KN)	Punch Pressure (MPa)	Punch Speed (mm/s)
200	4	60	3	30	3.0	20

The lubrication state of the material can be divided into fluid lubrication ($\mu \leq 0.03$), mixed lubrication ($0.03 < \mu \leq 0.1$), boundary lubrication ($0.1 < \mu < 0.3$) and dry friction ($\mu > 0.3$). During the actual stamping process, most of the sheet metal interface friction states are boundary lubrication and mixed lubrication. Two groups of constant friction coefficient and variable friction coefficient modified friction models with a friction coefficient of 0.08 (mixed lubrication) and an optimal combination friction coefficient of 0.12 (boundary lubrication) were selected for the simulation. The simulated thickness distributions of the U-bend under different friction coefficients are shown in Figure 9.
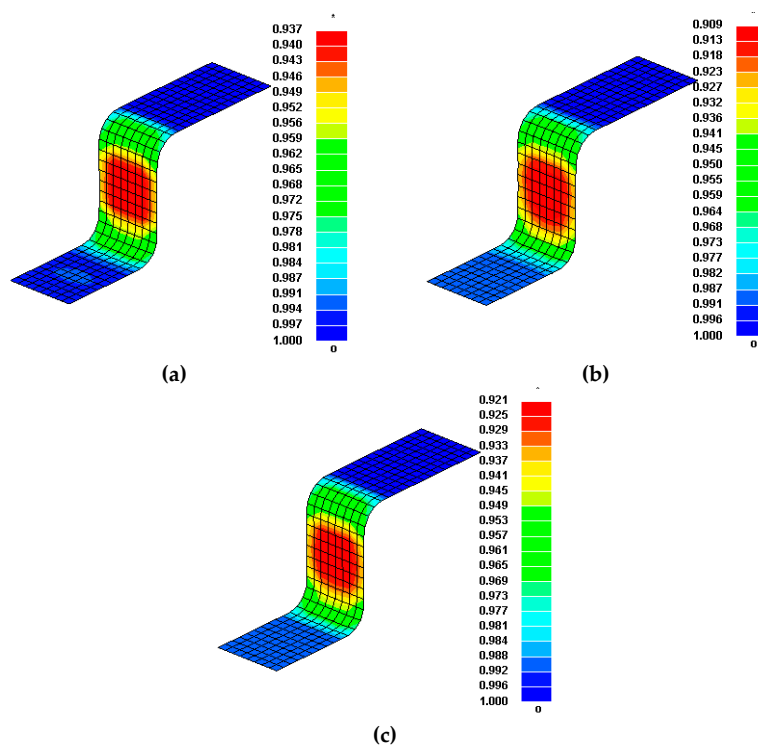

Figure 9. Thickness distributions under different friction coefficients of U-bending. (**a**) $\mu = 0.08$; (**b**) $\mu = 0.12$; (**c**) Variable friction coefficient model.

The warming stamping U-bend part test device was developed by the metal forming Laboratory of Jiangsu University, and it includes a temperature detection and control system, induction-heating furnace, U-shaped hot stamping die with water cooling, a hydraulic press, etc., as shown in Figure 10b. The hot stamping temperature control system collects the sheet temperature and die surface temperature warming by using an infrared thermometer, and it controls the temperature by water cooling. After being heated by the induction furnace, it is quickly sent to the hot die.

(a)   **(b)**
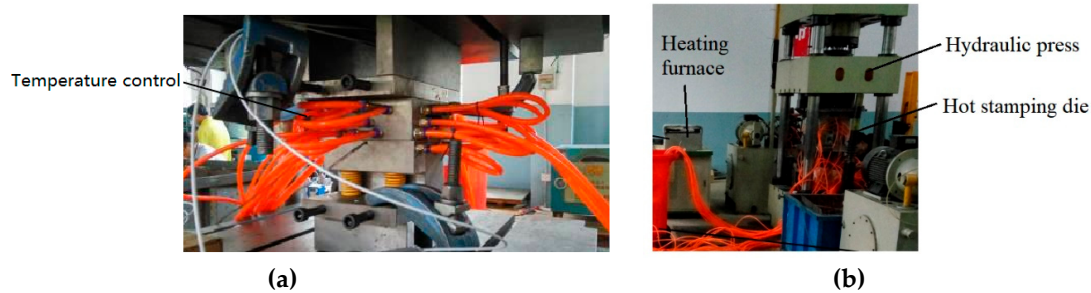
Figure 10. Friction coefficient curve under different loads and function fitting curve: (**a**) Warming stamping mold; (**b**) Test device for hot stamping U-shaped parts.

The working parts of the die are made of H13 steel and do not need to be heated, and there is a cooling water pipe for cooling, as shown in Figure 10a. The speed and load of die movement are controlled by a hydraulic press.

The U-bend warming stamping parts are shown in Figure 11a. The thickness of the actual stamping parts was measured through the use of an ultrasonic thickness gauge, and the measuring point was the symmetrical center of the sheet width direction. The distribution curves of the plate thickness were determined by the constant friction coefficient, and the modified friction model and test are shown in Figure 11b.

(a)

(b)

(c)
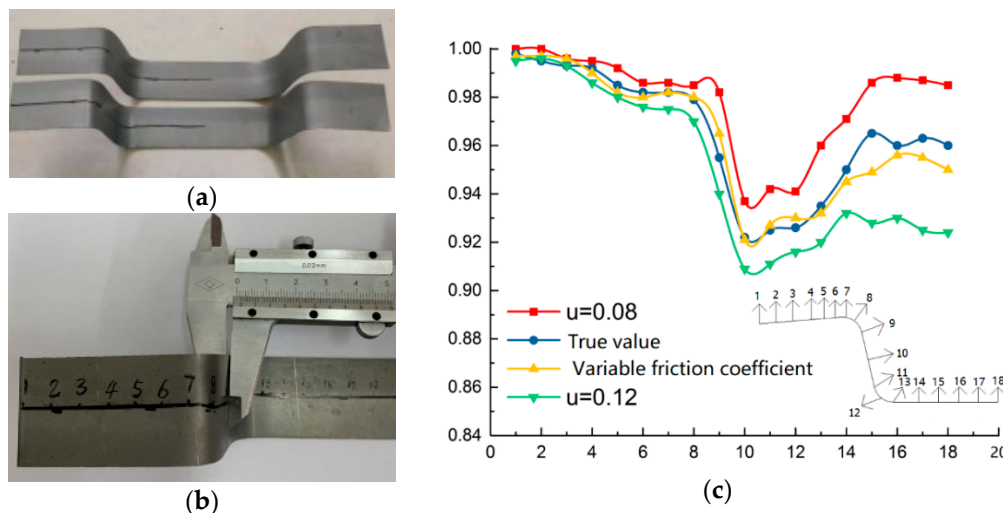
Figure 11. Friction coefficient curve under different loads and function fitting curve: (**a**) Warming stamping mold; (**b**) U-bend parts and thickness measurement; (**c**) Thickness distribution curve under different conditions.

Under an optimal combination of process parameters, when the stamping speed is 20 mm/s and the blank holder force is 30 KN, a constant friction coefficient of 0.12 and the variable friction coefficient model were selected to simulate the warm forming of 6111 aluminum alloy, and the spring-back of the U-bend was measured (diagrams of the spring-back angle and measurement are shown in

Figure 12). In order to reduce the measurement error of the actual spring-back angle, the average values of five actual U-bend parts were taken as the effective spring-back angle. According to the above measurements and calculation formula of the variable friction coefficient model, the spring-back angles $\Delta\theta_1$ and $\Delta\theta_2$ of the actual stamping parts were 6.5° and −6.8°. The spring-back angle reflects the spring-back deformation degree of parts after warm forming. In the post-processing of DYNAFORM, the spring-back angle under the constant friction coefficient and variable friction coefficient model were measured. The measurement results are shown in Table 5.

(a)　　　　　　　　　　　　　　　　　　　　　　　　**(b)**
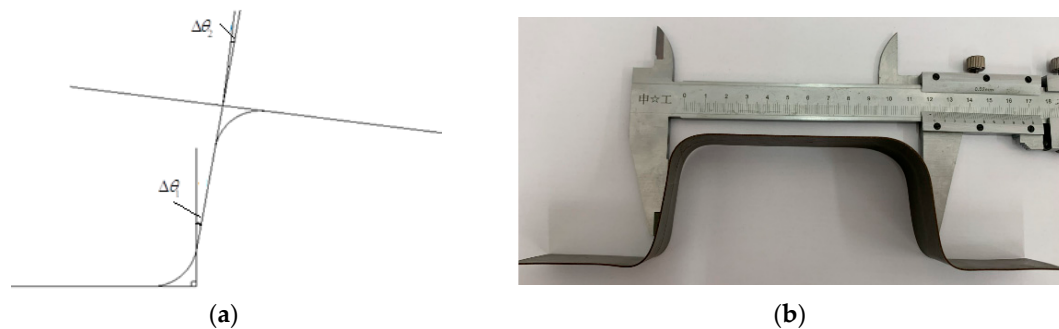
Figure 12. Friction coefficient curve under different loads and function fitting curve: (**a**) Spring-back angle; (**b**) True spring-back measurement.

As seen in Table 6 the predicted values of the spring-back angles $\Delta\theta_1$ and $\Delta\theta_2$ based on the constant friction coefficient model were 5.2° and 5.9°, and the errors between the predicted value of the spring-back angle and the actual stamping measurement were 20% and 9.2%. The predicted values of the spring-back angles $\Delta\theta_1$ and $\Delta\theta_2$ were −5.4° and −6.2°, respectively, obtained by using the modified friction model, and the errors between them and the actual stamping measurement were 9.2% and 8.8%.

Table 6. Comparison of simulation and test results of the rebound angle.

Spring-Back/(°)	$\Delta\theta_1$	$\Delta\theta_2$
True value	6.5	−6.8
Constant friction coefficient	5.2 (Error, 20%)	−5.4 (Error, 20.6%)
Variable friction coefficient	5.9 (Error, 9.2%)	−6.2 (Error, 8.8%)

Therefore, the prediction of the spring-back angle of sheet metal forming based on the modified friction model is closer to the actual measurement results and can reflect the characteristics of sheet metal forming more realistically.

5. Conclusions

The effects of temperature, sliding speed and normal load on friction and wear properties resulting from friction between 6111 aluminum alloy and H13 die steel were studied by using a CFT-I friction tester under different lubrication conditions. The surface morphology of 6111 aluminum alloy under different experimental conditions was observed and analyzed through an optical microscope, and the influence mechanism of different experimental parameters affecting the friction coefficient was studied from a microscopic perspective. From the analysis of experimental data, variable friction coefficient models based on sliding speed and normal load were established using the Origin software, and the validity of the models was verified. The conclusions are as follows.

(1) Under different process parameters, the friction coefficient shows rapid fluctuation during the running-in stage and relatively stable levels of fluctuation in the later stage. With the increase in time, the friction coefficient first increases sharply and then decreases to a relatively stable state.

(2) The friction coefficient increases with the increase in temperature, from room temperature to 200 °C, and the increasing trend of the friction coefficient becomes slower with the continuous increase in temperature; the influence of different temperatures on the hardness of 6111 aluminum alloy is not pronounced. According to the observation of surface micro-morphology, the number of furrows on the 6111 aluminum alloy surface is limited, the surface is relatively smooth and the surface morphology is better at 200 °C.

(3) When the temperature is 200 °C and the load is 20 N, the friction coefficient decreases with the increase in sliding speed. According to the analysis, the variable friction coefficient model of sliding speed was established, and the errors of the model are all less than 8%, which shows the effectiveness of the variable friction coefficient model.

(4) The results show that the friction coefficient decreases with the increase in normal load when the temperature is 200 °C and the sliding speed is 30 mm/s. When the interface load is greater than 30 N, the decreasing trend gradually slows down. The morphology observations show that with the increase in the interface load, the scratches on the surface of 6111 aluminum alloy clearly increase and deepen, and surface exfoliation occurs.

(5) With the optimal process parameters, a stamping simulation of typical U-bending parts was carried out by using finite element analysis software and the variable friction coefficient model established by the friction test. The thickness distribution simulation results under a mixed lubrication state and a boundary lubrication state were compared with the actual U-shaped stamping parts. Through the comparison of thickness distribution, it is observed that the simulation results for the thickness distribution based on the variable friction coefficient model are close to the actual measured values. Through the analysis of the spring-back angle, it is also observed that the spring-back measurement error of the variable friction coefficient model is smaller than that of the constant friction coefficient model. Therefore, the variable friction coefficient model improves simulation accuracy.

Author Contributions: Conceptualization, S.D.; methodology, S.D.; software, S.D.; advisors, X.W. and L.W.; formal analysis, J.X.; data curation, S.D.; writing—original draft preparation, S.D.; writing—review and editing, S.D.; funding acquisition, J.X. All authors have read and agreed to the published version of the manuscript.

Conflicts of Interest: The authors declare no conflict of interest.

References

1. Hosseini-Tehrani, P.; Nikahd, M. Two materials S-frame representation for improving crashworthiness and lightening. *Thin Walled Struct.* **2006**, *44*, 407–414. [CrossRef]
2. Kim, H.-J.; McMillan, C.; Keoleian, G.A. Greenhouse gas emissions payback for lightweighted vehicles using aluminum and high-strength steel. *J. Ind. Ecol.* **2010**, *14*, 929–946.
3. Unbo, J.; Anders, U. A parametric study for the structural behavior of a Light-weight deck. *Eng. Struct.* **2004**, *26*, 963–977.
4. Fakir, E.; Omer, D.S.; Stone, I. Solution heat treatment, forming and in-die quenching of a commercial sheet magnesium alloy into a complex-shaped component: Experimentation and FE simulation. *Key Eng. Mater.* **2014**, *622*, 596–602. [CrossRef]
5. Finch, D.M.; Wilson, S.P.; Dorn, J.E. Deep drawing aluminum alloy at elevated temperatures part I-deep drawing cylindrical cups. *Trans. ASM* **1946**, *1*, 254–289.
6. Finch, D.M.; Wilson, S.P.; Dorn, J.E. Deep drawing aluminum alloy at elevated temperatures part II-deep drawing boxes. *Trans. ASM* **1946**, *1*, 290–310.
7. Ayres, R.A.; Wenner, M.L. Strain and strain-rate hardening effects in punch stretching of 5182-0 aluminum at elevated temperatures. *Metall. Trans.* **1979**, *10*, 41–46. [CrossRef]
8. Li, D.; Ghosh, A. Tensile deformation behavior of aluminum alloys at warm forming temperatures. *Mater. Sci. Eng. A* **2003**, *352*, 279–286. [CrossRef]
9. Simões, V.M.; Oliveira, M.C.; Laurent, H.; Menezes, L.F. The punch speed influence on warm forming and springback of two Al-Mg-Si alloys. *J. Manuf. Process.* **2019**, *38*, 266–278. [CrossRef]

10. Lee, B.H.; Keum, Y.T.; Wagoner, R.H. Modeling of the friction caused by lubrication and surface roughness in sheet metal forming. *J. Mater. Process. Technol.* **2002**, *130*, 60–63. [CrossRef]

11. Im, Y.T.; Kang, S.H.; Cheon, J.S. Finite element investigation of friction condition in a backward extrusion of aluminum alloy. *Trans. ASME J. Manuf. Sci. Eng.* **2003**, *125*, 378–383. [CrossRef]

12. Zhao, Y.Z.; Wang, K.; Wang, W.R.; Wei, X.C. Application of variable friction coefficient model in forming of advanced high-strength steel. *J. Shanghai Jiaotong Univ.* **2015**, *49*, 1446–1451.

13. Dou, S.S.; Xia, J.S. Analysis of sheet metal forming (stamping process): A study of the variable friction coefficient on 5052 aluminum alloy. *METALS* **2019**, *9*, 853. [CrossRef]

14. ISO 12004-2:2008. *Metallic Materials—Sheet and Strip—Determination of Forming-Limit Curves—Part 2: Determination of Forming-Limit Curves in the Laboratory*; ICS: Geneva, Switzerland, 2008.

15. Yoshikiyo, T.; Toru, I.; Ken-ichi, M. FE forming analysis with nonlinear friction coefficient model considering contact pressure, sliding velocity and sliding length. *J. Mater. Process. Technol.* **2016**, *227*, 161–168.

16. Erding, W.; Renbo, S.; Xiong, W.M. Effect of tempering temperature on microstructuresand wear behavior of a 500 HB grade wear-resistant steel. *Metals* **2019**, *9*, 45.

17. Zhang, D.H.; Bai, D.P.; Liu, J.B. Formability Behaviors of 2a12 thin-wall part based on dynaform and stamping experiment. *Compos. Part B Eng.* **2013**, *55*, 591–598. [CrossRef]

18. Boyer, H.E. *Atlas of Stress-Strain Curves*; ASM International: Cleveland, OH, USA, 2002; p. 235270.

19. Schey, J. *Tribology in Metalworking: Lubrication, Friction and Wear*; American Society for Metal: Metal Park, OH, USA, 1983; pp. 125–150.